DOI: 10.1002/anie.200801629

Chiral Hybrid Gelator

Chiral Strandberg-Type Molybdates $[(RPO_3)_2Mo_5O_{15}]^{2-}$ as Molecular Gelators: Self-Assembled Fibrillar Nanostructures with Enhanced Optical Activity**

Mauro Carraro, Andrea Sartorel, Gianfranco Scorrano, Chiara Maccato, Michael H. Dickman, Ulrich Kortz,* and Marcella Bonchio**

Complementary assembly of organic and inorganic molecular components is a powerful strategy for the synthesis of novel hybrid frameworks with extended architectures and functional applications in storage, separation, and catalysis.[1]

Organophosphonate metal oxide phases $[M_xO_y(RPO_3)_z]$ have been successfully exploited for the design of hybrid materials in which the organic residues decorate the surfaces of the inorganic domains and for controlling the solid-state arrangement of multiple M/O/P layers.[2] In particular, the Strandberg-type polyoxomolybdate subunit $[(RPO_3)_2Mo_5O_{15}]^{4-}$ is ubiquitous in this structural chemistry.[3,4] The presence of two organic stereo-electronic effectors per molecule is a valuable tool for modulating the physicochemical properties, morphology, and performance of the resulting material.[2,4–6] In this respect, the development of optically active frameworks by incorporation of enantiopure organic components is a major research goal.[7] Moreover, the expression of chirality on the supramolecular, nano/micrometer scale, giving rise to coiled/twisted hybrid superstructures, still poses a formidable intellectual and experimental challenge in the field of molecular recognition and self-assembly.[8] Herein we report on a unique polyoxometalate (POM)-based soft material, constructed from chiral aminophosphonate pentamolybdate units $[(R^*PO_3)_2Mo_5O_{15}]^{2-}$, which undergo rodlike self-assembly by hydrogen bonding and evolve to a hierarchical architecture of entangled fibers that ultimately results in solvent gelation. The Strandberg-type POM subunit is readily synthesized[4] in water at pH 3, from sodium molybdate and enantiopure aminoalkyl phosphonic acids $R^*PO_3H_2$ (Figure 1). The pentamolybdate core

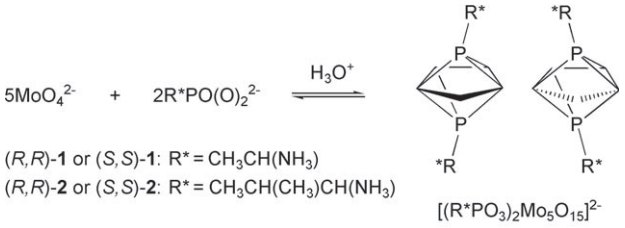

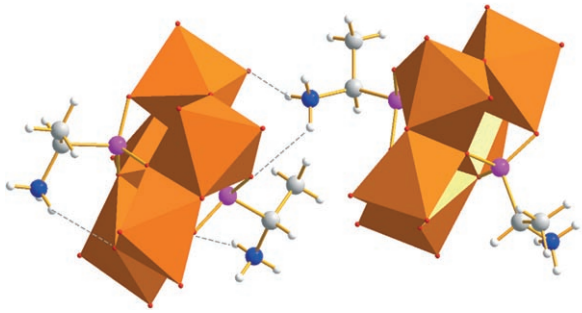

Figure 1. Top: Schematic synthesis and "envelope" representation of the polyanions $[(R^*PO_3)_2Mo_5O_{15}]^{2-}$. Bottom: Polyhedral/ball-and-stick representation of the two diastereomeric forms of (*R*,*R*)-**1**, crystallized as Rb salts. MoO_6 octahedra orange, O red, P magenta, C gray, N blue, H white. Inter- and intramolecular hydrogen bonds with distances in the range of 2.841(7)–3.307(8) Å are highlighted.[20]

is assembled in solution most likely by a template effect of the two phosphonate ligands attached on opposite, external sides of the Mo_5O_{15} ring through three oxygen atoms in a trigonal-pyramidal fashion (Figure 1). Each molybdenum center displays distorted octahedral coordination with connection to the phosphonate moiety by two fairly long Mo–O(P) bonds (2.199(5)–2.471(5) Å), both of which are *trans* to a terminal M=O group. The nonplanar arrangement of the five MoO_6 octahedra, with four edge and one corner junctions, yields enantiomorphic Mo_5O_{15} rings with formal "Δ" or "Λ" helical handedness. Indeed, the X-ray crystallographic analysis of $Rb_2[(R,R)\text{-}\{CH_3CH(NH_3)PO_3\}_2Mo_5O_{15}]\cdot 2H_2O$ (Rb-(*R*,*R*)-**1**) shows both Δ and Λ diastereomeric forms in the unit cell (Figure 1).

The amino group of each phosphonate ligand is protonated, and thus a zwitterionic structure and a network of intra-

[*] Dr. M. Carraro, Dr. A. Sartorel, Prof. G. Scorrano, Dr. C. Maccato, Dr. M. Bonchio
ITM-CNR and Department of Chemical Sciences
University of Padova
via Marzolo 1, 35131 Padova (Italy)
Fax: (+39) 049-827-5239
E-mail: mauro.carraro@unipd.it
marcella.bonchio@unipd.it
Dr. M. H. Dickman, Prof. U. Kortz
School of Engineering and Science, Jacobs University
P.O. Box 750 561, 28725 Bremen (Germany)
Fax: (+49) 421-200-3229
E-mail: u.kortz@jacobs-university.de

[**] Financial support from CNR, MIUR (FIRB CAMERE-RBNE03JCR5), and the ESF COST D29, D40 action are gratefully acknowledged. U.K. thanks Jacobs University and the Fonds der Chemischen Industrie for research support. We thank Dr. Luca Baù for TEM and EDX analyses.

Supporting information for this article is available on the WWW under http://dx.doi.org/10.1002/anie.200801629.

and intermolecular hydrogen bonds with the anionic polyoxygenated inorganic surface are generated.[3,9] The interplay of these multiple ionic-type interactions is expected to control the solution self-assembly of the discrete POM units, as well as the surface mobility of the organic chelates and the morphology of the extended structures.[10,11] Density functional calculations, including relativistic and solvent effects, were performed to evaluate the impact of hydrogen bonding on the geometries and energies of the (*R*,*R*)-**1** conformers in water.[11] The latter originate from rotation of the two protonated amino pendants, each of which acts as a monofunctional hydrogen-bond donor towards the Mo_5O_{15} multiple-acceptor surface according to the calculated electrostatic potential map (see Supporting Information). On ligand rotation, an extended domain of stabilizing interactions results as a function of the N_i-C_i-P_i-O_i dihedral angles Φ_i with $i = 1$ or 2 (blue zone in Figure 2, Φ_i in the range −180 to −70 and 120 to 180°). Indeed, the concurrent interaction of each NH_3^+ group with three proximal oxygen sites (two terminal M=O and one bridging Mo-O-Mo groups) on opposite sides of the Mo_5 ring results in two independent intramolecular hydrogen bonds, each of which provides an energy gain of 6 kcal mol^{-1}.[12]

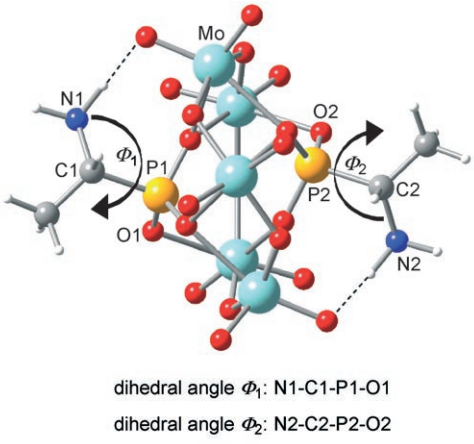

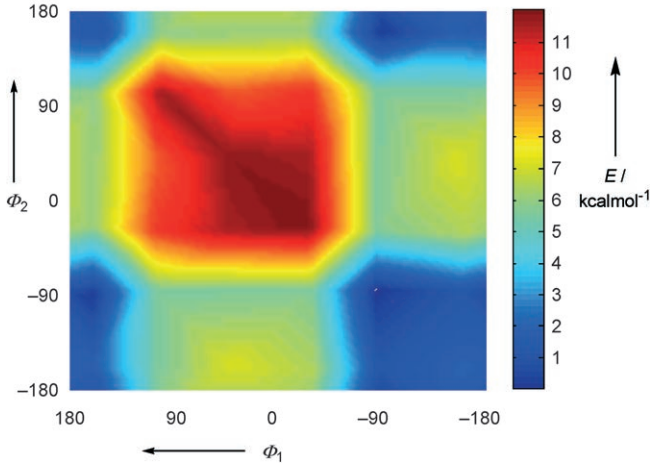

Figure 2. Top: most stable conformer of (*R*,Δ,*R*)-**1** ($\Phi_1 = -84.2$, $\Phi_2 = -84.4$). Bottom: energy–conformation analysis for (*R*,Δ,*R*)-**1**: energy is plotted as a function of Φ_1 and Φ_2 dihedral angles associated with $CH_3CH(NH_3)$ rotation; the picture was obtained by extrapolating 36 conformers (see Supporting Information). Stability regions are defined by Φ_i ranging from −180 to −70 and from 120 to 180°.

These phenomena are pivotal for the stability of the molecular polyanions and for their anisotropic aggregation in one or two dimensions to form elongated superstructures. Thus, the solution equilibria were investigated by NMR spectroscopy and induced circular dichroism (ICD) in aqueous and in organic media. Polyanions **1** and **2** (R = $CH_3CH(CH_3)CH(NH_3)$), the achiral analogues **3** (R = $NH_3CH_2CH_2$), and **4** (R = CH_3CH_2), typically exhibit a single $^{31}P\{H\}$ NMR resonance both in D_2O and [D_6]DMSO (Table S2, Supporting Information).[10] While 10–40% dissociation occurs in water (pH 3.5) by release of the ligand with formation of other phosphonomolybdates (broad ^{31}P NMR signal at $\delta = 16$–19 ppm),[10] remarkable stability is observed in DMSO. This evidence points to different POM/ligand dynamics in water and in organic media, driven by the stability of the ionic-type hydrogen bonding.[9,13] Therefore, experiments were designed to assess ligand scrambling both in aqueous and in organic media.[14]

Increased addition of (*S*)-$CH_3CH(NH_2)PO_3H_2$ ((*S*)-AEPA) to (*R*,*R*)-**1** in D_2O leads to the formation of pseudo-*meso*, heterochiral complex (*R*,*S*)-**1** and enantiomeric (*S*,*S*)-**1** in statistical distribution. Monitoring this by $^{31}P\{H\}$ NMR shows progressive buildup of a new signal at $\delta = 22.4$ ppm, attributed to (*R*,*S*)-**1**, which reaches its maximum intensity at equimolar (*R*)/(*S*)-AEPA ratio (Figure 3A). Monitoring by ICD provided a consistent picture, whereby transformation of (*R*,*R*)-**1** into enantiomeric (*S*,*S*)-**1** on addition of (*S*)-AEPA leads to mirror-symmetrical chiroptical traces with distinct Cotton effects, in the region of the Mo–O charge-transfer bands, up to 350 nm ($\theta_{max} = 2 \times 10^4$ deg cm^2 dmol^{-1}, Figure 3B, curves 1–6).[15] Then we performed analogous studies in [D_6]DMSO by mixing equimolar amounts of **1**–**4** with (*R*,*R*)-**2** in separate experiments. In all cases, equilibration to the crossed-type adduct is not observable, but it occurs steadily on addition of increasing amounts of water to the DMSO solution (Figure 4). The extent of ligand scrambling *x* as a function of the percentage of H_2O in DMSO provides a direct estimate of the sensitivity of the system to solvent composition. Analysis of the curves in Figure 4A ranks the diverse POMs in the order of increasing stability: **4** < **1** < **3** < **2**.[16] This observation highlights the prominent role of the charged amino substituent, which "freezes" phosphonate exchange within the hydrogen-bonded structure. Accordingly, the latter is strongly affected by water addition.

The reverse approach, that is, addition of an appropriate organic solvent with lowering of the medium polarity,[8c] is expected to stabilize hydrogen bonding, which is likely the primary driving force for formation of unprecedented rodlike aggregates, and induce gelator properties.[8c] On addition of EtOH to an aqueous solution of (*R*,*R*)-**1** (27 mM, pH 3.5), the latter changes to a stable, semitransparent gel phase starting at about 90:10 EtOH/H_2O ratio, and very efficient entrapment of the solvent molecules occurs with about 0.2 wt% of the molecular gelator (see Supporting Information). The gelation process can also be observed with dioxane, *i*PrOH, *t*BuOH, THF, and hexafluoro-2-propanol, while in other

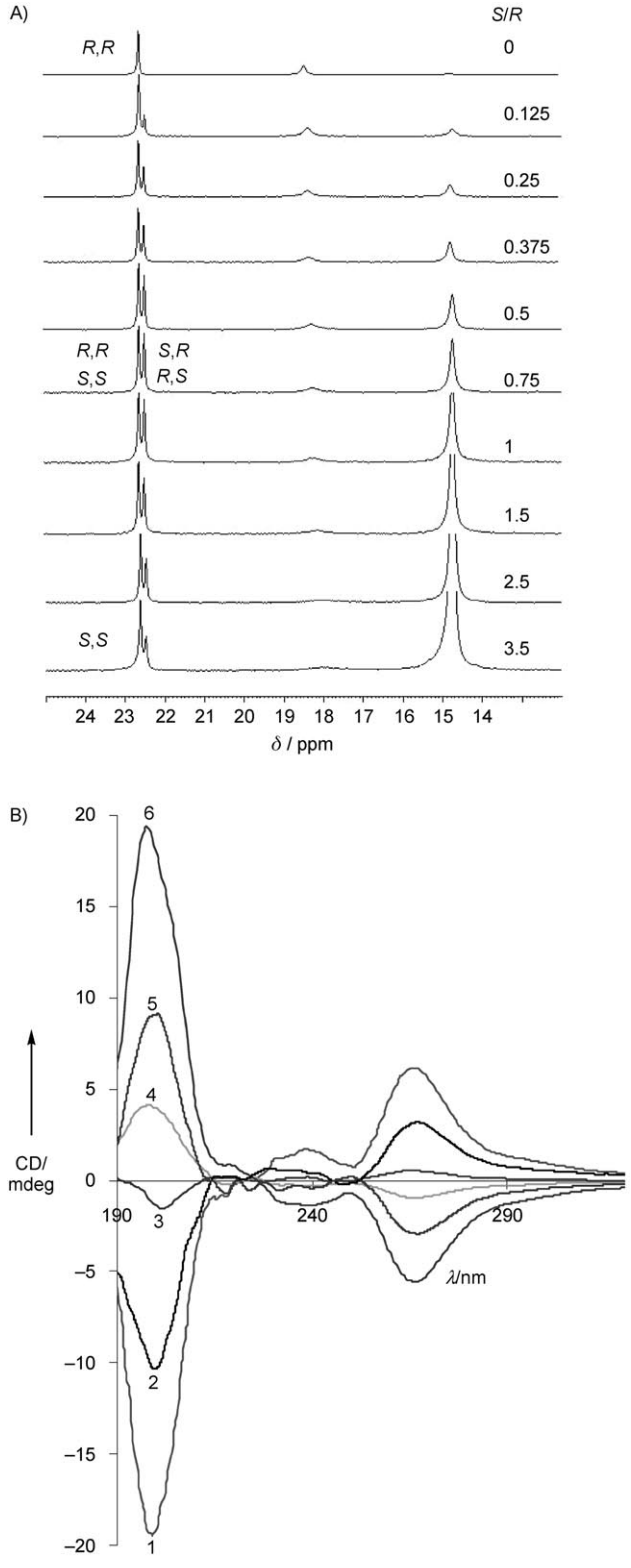

Figure 3. A) $^{31}P\{H\}$ NMR (D_2O, 301 K) spectra of (*R*,*R*)-**1** (3.6 mmol L^{-1}) in the presence of an increasing molar ratio of (*S*)-AEPA. B) ICD spectra of (*R*,*R*)-**1.** Starting concentration 7.78×10^{-5} mol L^{-1} in H_2O. 1) (*R*,*R*)-**1** + 5 equiv (*R*)-AEPA; 2) (*R*,*R*)-**1**. 3) (*R*,*R*)-**1** + 2 equiv (*S*)-AEPA. 4) (*R*,*R*)-**1** + 5 equiv (*S*)-AEPA. 5) (*S*,*S*)-**1**. 6) (*S*,*S*)-**1** + 5 equiv (*S*)-AEPA.

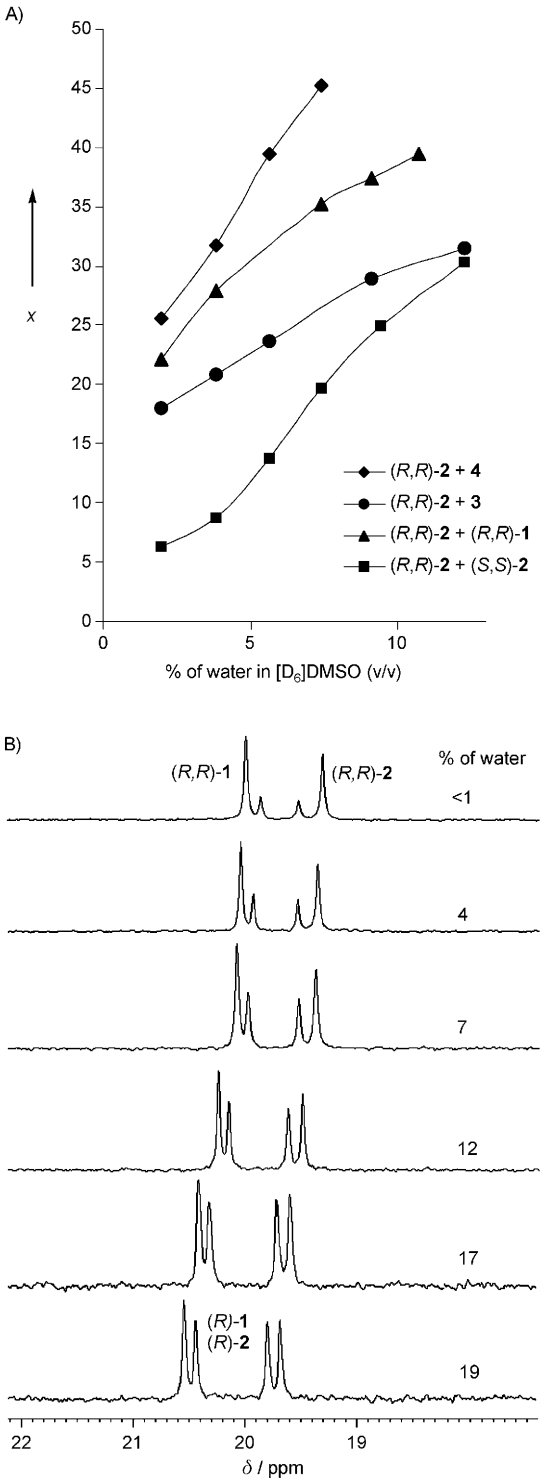

Figure 4. A) Extent of ligand scrambling *x* as a function of the percentage of H_2O in DMSO after mixing of **1**–**4** with (*R*,*R*)-**2**. Data obtained from integration of $^{31}P\{H\}$ NMR spectrum ([D_6]DMSO, 301 K), with $x = [AB]/([AB]+[AA]+[BB])\times100$, where AA and BB are the homoligated phosphonates and AB the mixed-type derivative. B) $^{31}P\{H\}$ NMR ([D_6]DMSO, 301 K) spectra of an equimolar mixture of (*R*,*R*)-**1** (3.6 mmol L^{-1}) and (*R*,*R*)-**2** (3.6 mmol L^{-1}) with increasing percentage of water.

solvents, such as *N*,*N*-dimethylformamide (DMF), dimethyl sulfoxide (DMSO), and CH_3CN, the title POM fails to form gels, regardless of its concentration. Similar behavior is observed for (*R*,*R*)-**2**. Evidence of the molecular organization of the POM-based gel is provided by scanning electron microscopy (SEM) and transmission electron microscopy (TEM), performed on dried samples of the soft material. The gel network consists of quite homogeneous fibers with diameters between 20 and 40 nm and lengths of several micrometers (up to 5 μm), which split or intertwine to form an entangled 3D network (see Supporting Information). High-resolution TEM images of single fibers show an ordered substructure, with parallel rows about 2 nm in width, in agreement with the packing of the hydrogen-bonded POM subunits observed in the solid state (Figure 5).[17]

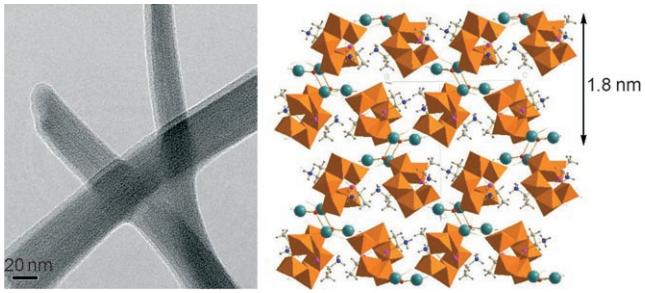

Figure 5. Left: TEM analysis of Na-(*R*,*R*)-**1**. Right: crystal packing diagram for Rb-(*R*,*R*)-**1**. MoO_6 octahedra orange, O red, P magenta, C gray, N blue, H white, Rb azure..

The sol–gel transition is accompanied by strong enhancement of the ICD features of the gel phase, which evolve to multiple dichroic bands with molar ellipticity θ_{max} greater than 10^5 deg cm^2 dmol^{-1}, one order of magnitude higher than the value in aqueous solution, ascribable to the isolated molecules (Figure 6).[7,18]

This phenomenon is associated with expression of chirality on the supramolecular scale, induced by the molecular POM gelator on the morphology of the self-assembled fiber.[7] Indeed, the supramolecular organization of (*R*,*R*)-**1** results in twisted fibrils with a right-handed helical structure and a regular pitch of about 150 nm (SEM image in Figure 6).[8] In conclusion, these results pave the way to the design of novel and chiral POM-based hybrids stabilized by multiple non-covalent interactions between the organic and inorganic molecular domains. Moreover, it sheds light on phosphonate exchange dynamics that might be exploited for the association/recognition of biological targets in water,[19] as well as for the preparation of new chiral materials via soft-chemistry routes.

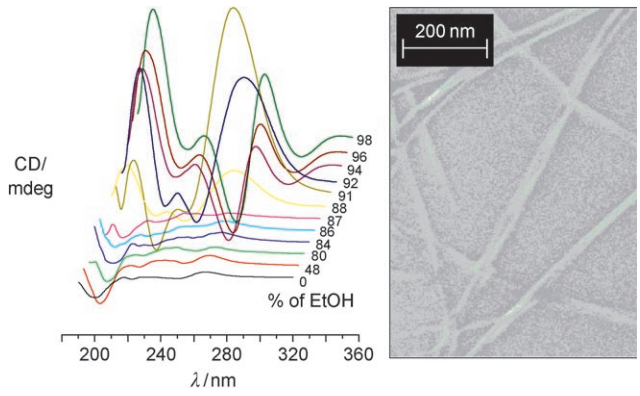

Figure 6. Left: ICD spectra of aqueous solutions of (*R*,*R*)-**1** (0.5 mmol L^{-1}, path length 1 mm) with increasing percentage of ethanol. Right: SEM image showing the twisted gel fibers with a pitch of about 150 nm.

Received: April 7, 2008
Published online: August 8, 2008

Keywords: gels · helical structures · nanostructures · polyoxometalates · self-assembly

[1] a) M. Antonietti, M. Niederberger, B. Smarsly, *Dalton Trans.* **2008**, 18–24; b) C. Sanchez, G. J. de A. A. Soler-Illia, F. T. Ribot, T. Lalot, C. R. Mayer, V. Cabuil, *Chem. Mater.* **2001**, *13*, 3061–3083; c) C. Streb, D. L. Long, L. Cronin, *Chem. Commun.* **2007**, 471–473.

[2] a) G. Cao, H.-G. Hong, T. E. Mallouk, *Acc. Chem. Res.* **1992**, *25*, 420–427; b) N. G. Armatas, D. G. Allis, A. Prosvirin, G. Carnutu, C. J. O'Connor, K. Dunbar, J. Zubieta, *Inorg. Chem.* **2008**, *47*, 832–854, and references therein.

[3] a) R. Strandberg, *Acta Chem. Scand.* **1973**, *27*, 1004–1018; b) W. Kwak, M. T. Pope, T. F. Scully, *J. Am. Chem. Soc.* **1975**, *97*, 5735–5738; c) J. K. Stalick, C. O. Quicksall, *Inorg. Chem.* **1976**, *15*, 1577–1584.

[4] a) U. Kortz, C. Marquer, R. Thouvenot, M. Nierlich, *Inorg. Chem.* **2003**, *42*, 1158–1162; b) E. V. Chubarova, C. Klöck, M. H. Dickman, U. Kortz, *J. Cluster Sci.* **2007**, *18*, 697–710.

[5] a) M. Bonchio, M. Carraro, G. Scorrano, A. Bagno, *Adv. Synth. Catal.* **2004**, *346*, 648–654; b) M. Carraro, L. Sandei, A. Sartorel, G. Scorrano, M. Bonchio, *Org. Lett.* **2006**, *8*, 3671–3674; c) S. Berardi, M. Bonchio, M. Carraro, V. Conte, A. Sartorel, G. Scorrano, *J. Org. Chem.* **2007**, *72*, 8954–8957.

[6] Y.-F. Song, N. McMillan, D.-L. Long, J. Thiel, Y. Ding, H. Chen, N. Gadegaard, L. Cronin, *Chem. Eur. J.* **2008**, *14*, 2349–2354.

[7] a) H. An, E. Wang, D. Xiao, Y. Li, Z. Su, L. Xu, *Angew. Chem.* **2006**, *118*, 918–922; *Angew. Chem. Int. Ed.* **2006**, *45*, 904–908; b) H. Tan, Y. Li, Z. Zhang, C. Qin, X. Wang, E. Wang, Z. Su, *J. Am. Chem. Soc.* **2007**, *129*, 10066–10067.

[8] a) A. Brizard, R. Oda, I. Huc, *Top. Curr. Chem.* **2005**, *256*, 167–218; b) T. Shimizu, M. Masuda, H. Minamikawa, *Chem. Rev.* **2005**, *105*, 1401–1443; c) J. Brinksma, B. L. Feringa, R. M. Kellogg, R. Vreeker, J. van Esch, *Langmuir* **2000**, *16*, 9249–9255.

[9] a) M. P. Lowe, J. C. Lockhart, G. A. Forsyth, W. Clegg, K. A. Fraser, *J. Chem. Soc. Dalton Trans.* **1995**, 145–152; b) T. Steiner, *Angew. Chem.* **2002**, *114*, 50–80; *Angew. Chem. Int. Ed.* **2002**, *41*, 48–76, and references therein.

[10] a) A. Yagasaki, I. Andersson, L. Pettersson, *Inorg. Chem.* **1987**, *26*, 3926–3933; b) D.-G. Lyxell, D. Boström, M. Hashimoto, L. Pettersson, *Acta Chem. Scand.* **1998**, *52*, 425–430; c) M. Hashimoto, I. Andersson, L. Pettersson, *Dalton Trans.* **2007**, 124–132.

[11] a) A. Sartorel, M. Carraro, A. Bagno, G. Scorrano, M. Bonchio, *Angew. Chem.* **2007**, *119*, 3319–3322; *Angew. Chem. Int. Ed.* **2007**, *46*, 3255–3258; b) A. Bagno, M. Bonchio, *Angew. Chem.* **2005**, *117*, 2059–2062; *Angew. Chem. Int. Ed.* **2005**, *44*, 2023–2026.

[12] The stabilization energy may be slightly underestimated for hydrogen bonds in DMSO. Similar results were observed for

(*R*,Λ,*R*)-**1**. An overall energy difference of less than 0.5 kcal mol^{-1} indicates that the two diastereoisomeric forms, (*R*,Δ,*R*)-**1** and (*R*,Λ,*R*)-**1**, are isoenergetic. Steric effects contribute to a minor extent to the stabilization of conformers, with maximum energy differences of 2 kcal mol^{-1} per ligand (see Supporting Information).

[13] The presence of intramolecular hydrogen bonding in [D_6]DMSO is proven by a ^{1}H NMR signal at 8 ppm, attributed to the ligated NH_3^+ group, which undergoes only a modest change (< 0.01 ppm) upon 15-fold dilution.

[14] Ligand exchange was monitored by integration of the appropriate ^{31}P{H} NMR singlets, which generally appear as isolated peaks for both the starting polyanions and the crossed-type adducts, that is, kinetics are slow on the NMR timescale (see Supporting Information).

[15] In the explored spectral region the CD signal of the free phosphonate is negligible (Figure S20, Supporting Information).

[16] At less than 10 % H_2O, kinetic effects are negligible as confirmed by variable temperature (VT) ^{31}P{H} NMR experiments.

[17] Energy-dispersive X-ray analysis shows a Mo/P atomic ratio of 2.33:1, in agreement with the expected POM structure.

[18] Reports on the chiroptical properties of POMs are still very rare: a) J. F. Garvey, M. T. Pope, *Inorg. Chem.* **1978**, *17*, 1115 – 1118; b) M. Lu, J. Kang, D. Wang, Z. Peng, *Inorg. Chem.* **2005**, *44*, 7711 – 7713; c) X. Fang, T. M. Anderson, C. L. Hill, *Angew. Chem.* **2005**, *117*, 3606 – 3610; *Angew. Chem. Int. Ed.* **2005**, *44*, 3540 – 3544; d) Y. Hou, X. Fang, C. L. Hill, *Chem. Eur. J.* **2007**, *13*, 9442 – 9447.

[19] a) D. E. Katsoulis, A. N. Lambrianidou, M. T. Pope, *Inorg. Chim. Acta* **1980**, *46*, L55 – L57; b) E. Ishikawa. T. Yamase, *J. Inorg. Biochem.* **2006**, *100*, 344 – 350.

[20] CCDC 684703 contains the supplementary crystallographic data for this paper. These data can be obtained free of charge from The Cambridge Crystallographic Data Centre via www.ccdc.cam.ac.uk/data_request/cif.

